

Geometric and electronic structures of SiO₂/Si(001) interfaces

Takahiro Yamasaki and Chioko Kaneta

Fujitsu Laboratories Corporation, 10-1 Morinosato-Wakamiya, Atsugi, Kanagawa 243-0197, Japan

Toshihiro Uchiyama* and Tsuyoshi Uda

Joint Research Center for Atom Technology, Angstrom Technology Partnership, 1-1-4 Higashi, Tsukuba, Ibaraki 305-0046, Japan

Kiyoyuki Terakura

Joint Research Center for Atom Technology, National Institute for Advanced Interdisciplinary Research, 1-1-4 Higashi, Tsukuba, Ibaraki 305-8562, Japan

(Received 9 March 2000; published 1 March 2001)

Interface structures of SiO₂/Si(001) are studied by using the first-principles molecular-dynamics method. Three crystalline phases of the SiO₂, cristobalite, quartz, and tridymite, are stacked on the Si(001) substrate and are fully relaxed. When the SiO₂ layer is very thin (~ 7 Å), the lowest-energy structure is the tridymite, followed by the quartz phase. As the SiO₂ layer becomes thicker (~ 15 Å), the quartz phase has lower energy than the tridymite phase. The cristobalite phase on Si(001) is unstable due to large lattice mismatch, and transforms into a different crystal structure. No defects appear at the interface after the successive bond breaking and rebonding, but the energy of the resulting structure is the highest irrespective of the thickness. Calculations of the local density of states show that the band-gap change occurs on the SiO₂ side, resulting in an effective decrease of the oxide thickness by 2–5 Å.

DOI: 10.1103/PhysRevB.63.115314

PACS number(s): 73.20.At, 68.35.Ct, 68.55.–a

I. INTRODUCTION

Today's VLSI (very large scale integration) technology is in need of an atomic scale understanding of issues arising from the miniaturization of silicon devices. Among these, the understanding and control of structural and electronic properties of the SiO₂/Si interface are the key subjects. Intensive studies have been made both experimentally and theoretically, and yet we are far from the final goal. Although SiO₂ insulating films on a Si(001) wafer are amorphous as a whole, several experimental reports^{1–4} suggested that some crystalline phases exist at a certain ratio in the dioxide region near the interface. Shimura *et al.*¹ proposed a structure model of pseudocristobalite, which explained well their specific features of x-ray diffraction. Ourmazd *et al.*³ observed the interfaces using high-resolution transmission electron microscopy, and proposed a tridymite model from an analysis of their microscopy images. The fraction of these kinds of crystalline phases, incorporated into an amorphous oxide layer, is expected to increase with decreasing oxide thickness. In this paper, we calculate the atomic and electronic structures of crystalline SiO₂ and Si(001) interfaces by the first-principles molecular-dynamics method, using three crystalline phases, namely, pseudocristobalite, quartz, and tridymite stacked on the Si(001) surface, with special emphasis on the relative stability against oxide thickness. Similar crystalline interfacial models were already studied theoretically. For example, Carniato *et al.*⁵ simulated the Si(001)/SiO₂ (tridymite) interface using the Monte Carlo method. Pasquarello *et al.*⁶ studied tridymite models by using the first-principles molecular-dynamics method. Kageshima and Shiraishi⁷ also simulated oxidation processes using the first-principles calculation, and found that a quartz structure can be obtained if Si atoms are removed from the

interface during oxidation. However, there have been no calculations for the thickness dependence of the relative stability of these three kinds of crystalline oxide phases. Very recently, Buckzo *et al.*⁸ performed calculations for Si-SiO₂-Si superstructures using the same three crystalline SiO₂ phases as ours. However, the SiO₂ layers are not thick enough to reveal variations of the oxide properties with increasing thickness.

In the present paper we aim to calculate how the conduction- and valence-band edges change at the interface, which is very important in estimating the dependence of leakage currents on the oxide thickness and on the applied gate voltages of metal-oxide-semiconductor (MOS) devices.

II. METHODOLOGY

The present calculation is based on the density-functional theory (DFT), and employs pseudopotentials (PP's) [a norm-conserving PP for Si and ultrasoft Vanderbilt PP's (Ref. 9) for O and H] and the plane-wave basis. The cutoff energies of the plane-wave expansion for wave functions and charge densities are 25 and 144 Ry, respectively. We add the generalized gradient correction¹⁰ to the local-density approximation for the exchange-correlation potential. Our optimized lattice constants of α quartz are larger than the experimental values by 2.3%, and the band gap is obtained to be 5.8 eV, which is the same as that in Ref. 11. The lattice constant of bulk Si in the diamond phase is obtained to be 5.46 Å, which is larger than the experimental value by 0.63%. Unit cells of our interface models contain a silicon substrate of 7 ML, a SiO₂ region ranging from 2 to 5 ML, and a vacuum region. The interface unit cell is Si(001)-(2×2) ($a=7.72$ Å) for the tridymite models, and Si(001)-($\sqrt{2}\times\sqrt{2}$) ($a=5.46$ Å) for other models. The c axis length of the unit cells is 29.95 Å in common. Surface and back surface dangling bonds are ter-

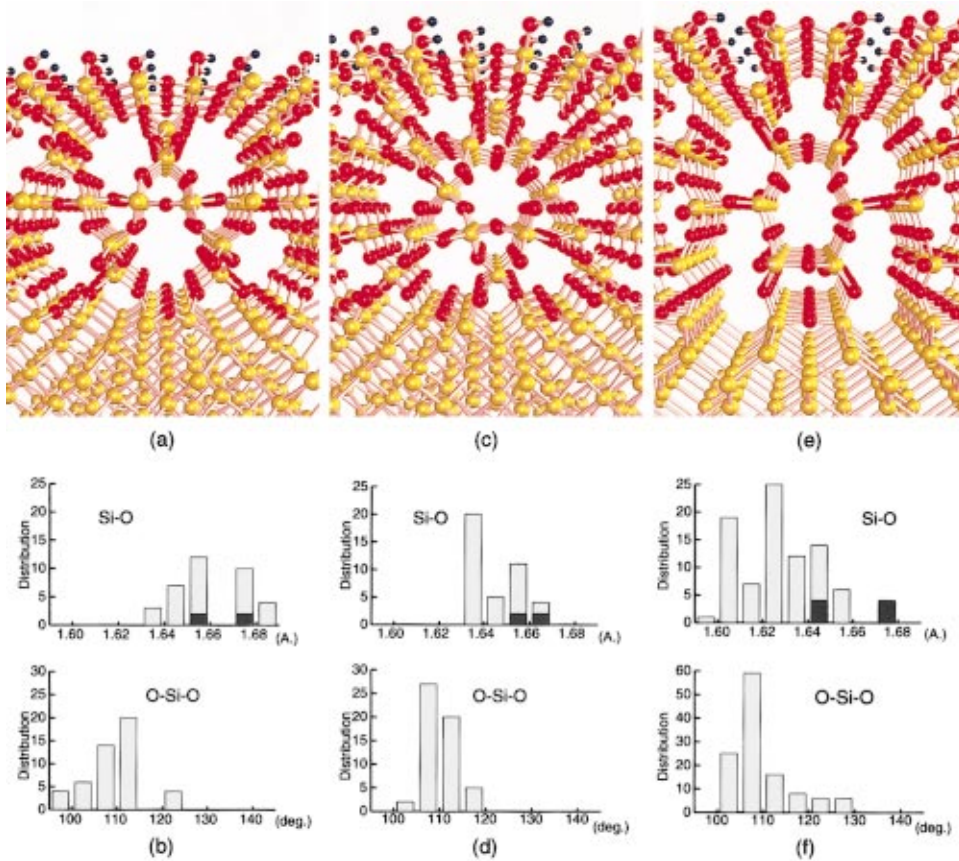


FIG. 1. (Color) (a) Optimized 4-ML type-*C* $\text{SiO}_2/\text{Si}(001)$ structure. Red, yellow, and blue balls are oxygen, silicon, and hydrogen atoms, respectively. (b) Distributions of Si-O bond lengths (upper) and O-Si-O bond angles (lower) for the type-*C* structure. In the histogram of the Si-O bond length, black parts are contributions from the Si-O bonds whose Si atoms belong to the substrate. (c) and (d) and (e) and (f) show 4.5-ML type-*Q* and the 5-ML type-*T* structures, respectively.

minated with H atoms. In the structure optimization processes, two bottom Si layers and H atoms stuck to the Si are fixed at equilibrium positions for a system composed of ten Si layers and surface termination H atoms. Four sampling k points are taken in the Brillouin zone for the smaller unit cell, and two k points for the larger one, to assure the same accuracy.

III. RESULTS AND DISCUSSION

We first examine the stability of the pseudocristobalite structure proposed by Shimura *et al.*,¹ with 4 ML stacked on the Si(001) surface. The unit cell contains 22 Si, 19 O, and six H atoms. The pseudocristobalite structure is compressed in lateral directions to match its lattice constant with that of Si(001), and is expanded along the normal direction to adjust the density. This structure is unstable because of largely distorted bond angles of O-Si-O. We found that it transforms into a completely different structure through a structure optimization process, where Si-O bond breaking and rebonding frequently take place, resulting in a tetrahedral Si-O network with no broken bonds both in the SiO_2 layers and at the interface. The final configuration is energetically more stable than the initial one by more than 6 eV per one SiO_2 . Figure 1(a) shows the final optimized structure. Hereafter for convenience we call this structure type *C* in this paper. As shown in Fig. 1(b), Si-O bond lengths and O-Si-O bond angles spread in the ranges of 1.63–1.69 Å and 98°–124°, respectively. The density of SiO_2 is 93% of our calculated value for the crystal α quartz. The SiO_2 part has fivefold,

sixfold, sevenfold, and eightfold Si-O rings, while the original cristobalite, the tridymite, and the α -quartz structures have only sixfold Si-O rings. Neglecting the distortions, the SiO_2 structure is considered to have a body-centered-tetragonal Bravais lattice containing four SiO_2 units in the primitive lattice.¹²

We, next, examine a 4.5-ML-thick quartz model. Since the surface of 4-ML SiO_2 in the quartz phase is rough, we use 23 Si, 21 O, and six H atoms for construction of a smooth surface, which nominally corresponds to 4.5 ML. Figures 1(c) and 1(d) show the optimized structure, which is called type *Q* for convenience, and the distributions of Si-O bond lengths and O-Si-O bond angles, respectively. This structure is estimated to be more stable than the type-*C* structure by subtracting the energy of 0.5 SiO_2 ML in the crystalline α -quartz phase. We will make a more quantitative comparison later by calculating the energies of thin SiO_2 models. The stability of the type-*Q* structure may be due to the smaller stress. The Si-O bond lengths and the O-Si-O bond angles concentrate in the ranges of 1.63–1.67 Å and 103°–118°, respectively, which are narrower than those of the type-*C* structure. The density of this SiO_2 region is 91% of our quartz value.

Third, we examine the tridymite model (type-*T* structure). We stacked 5-ML SiO_2 in the tridymite phase on the Si(001) with the 2×2 interfacial unit area. We introduced extra O atoms into substrate surface Si dimers like Pasquarello *et al.*⁶ Thus the unit cell contains 48 Si, 46 O, and 12 H atoms. In the optimized structure [Fig. 1(e)], although the Si-O net-

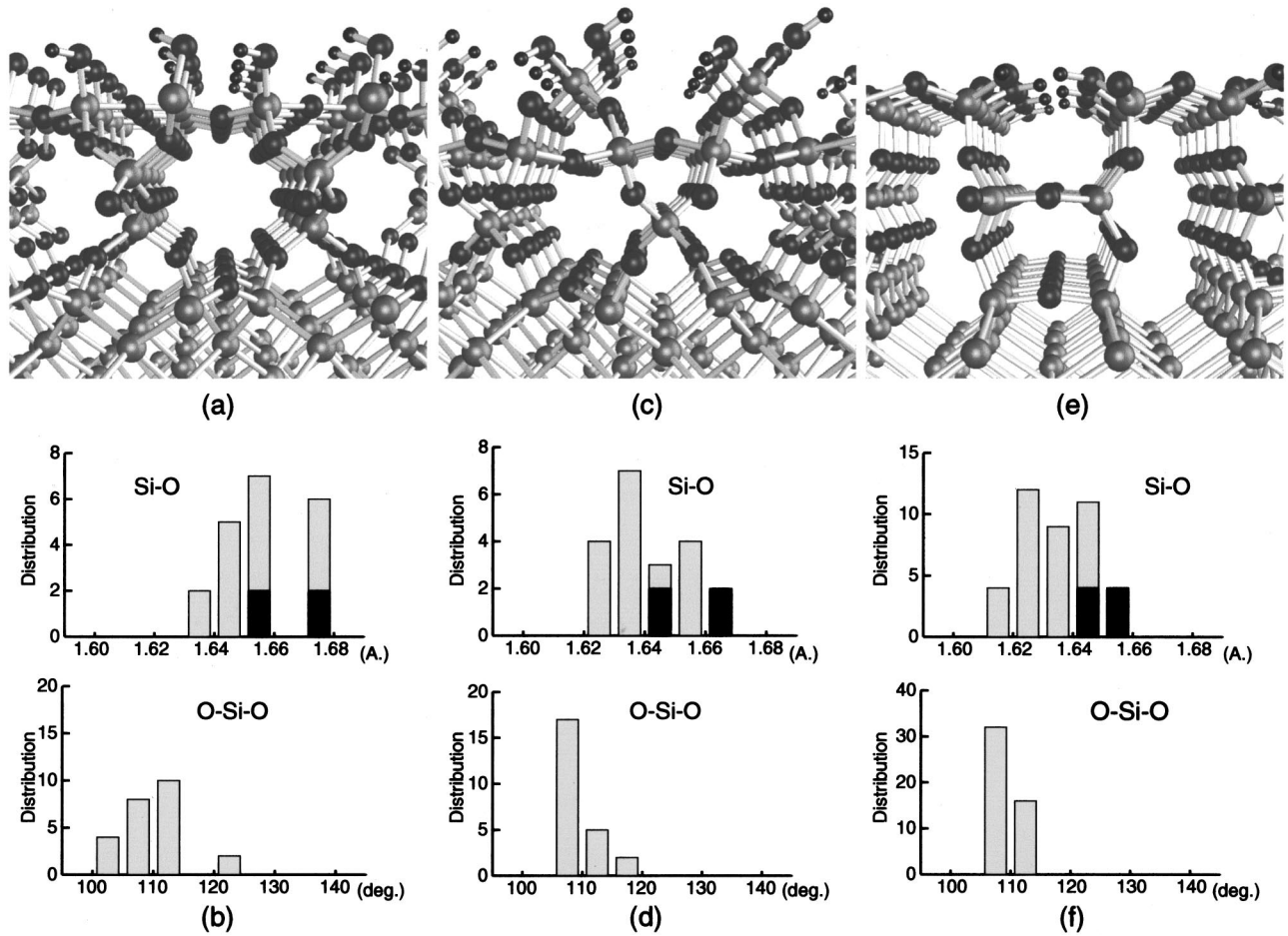


FIG. 2. (a) Optimized 2-ML type-*C* SiO₂/Si(001) structure. Larger black, larger gray, and small black balls are oxygen, silicon, and hydrogen atoms, respectively. (b) Distributions of Si-O bond lengths (upper) and O-Si-O bond angles (lower) for the type-*C* structure. In the histogram of the Si-O bond length, black parts are contributions from the Si-O bonds whose Si atoms belong to the substrate. (c) and (d) and (e) and (f) show 2-ML type-*Q* and the 2-ML type-*T* structures, respectively.

work geometry is the same as that of bulk tridymite, sixfold rings of the Si-O network are remarkably distorted. In this model the SiO₂ region is compressed compared to other models, with the density of SiO₂ being 95% of our quartz value. The Si-O bond lengths and Si-O-Si bond angles [Fig. 1(f)] spread in wider ranges than those of type-*Q* and -*C* structures, which means the thick type-*T* structure has larger stress than others. Nevertheless the energy of the type-*T* structure is estimated to be lower than that of the type-*C* structure.

In order to investigate the relative stability of the SiO₂ phases against the layer thickness, we also studied thin models with 2 ML. In these cases, the structures with equal SiO₂ layers can be constructed for the three phases, which makes it easy to compare the relative stability directly. Thin type-*C* and -*Q* structures have 18 Si, 11 O, and six H atoms in the unit cell, and a thin type-*T* structure has just doubled numbers of components. Optimized structures are shown in Figs. 2(a), 2(c), and 2(e). In contrast to the thicker cases, the type-*T* structure is the most stable among the three models (more stable than type *Q* by 0.24 eV/SiO₂, and than type *C* by 0.42 eV/SiO₂). Distributions of Si-O bond lengths and O-Si-O bond angles are also shown in Figs. 2(b), 2(d), and

2(f). The O-Si-O bond angle in the type-*C* structure spreads in a wider range than those of type-*Q* and -*T* structures, and the average Si-O bond length of the type-*C* structure is shifted to a larger value than those of the others by about 0.01 Å, which may be the reason why the thin type-*C* structure is the most unstable among the three models. On the other hand, it is hard to find the difference between type-*T* and -*Q* structures in the distributions of bond lengths and bond angles. However, it should be noted that, the type-*T* structures, a thin structure has much narrower distributions of bond lengths and angles than a thick one, while other structures have no such tendency.

To discuss the stability of three interfacial models in the thick region, we introduce the normalized total energy per interface Si(001)-(1×1) units relative to that of the bulk quartz of the same thickness, $E_{m,X}$ ($X=C, Q, \text{ or } T$), as functions of the number of SiO₂ layers (m). Assuming that the energy varies linearly with m between 2 and 5, in Fig. 3, we plot the relative energies of type-*C*, -*Q*, and -*T* structures, where the energy of $E_{2,Q}$ is set to be zero. As is clear from the figure, even if the $E_{m,X}$ has a slight nonlinearity upon thickness, the crossover from a type-*T* structure to a type-*Q* structure occurs at 3–4 ML. This observation does not nec-

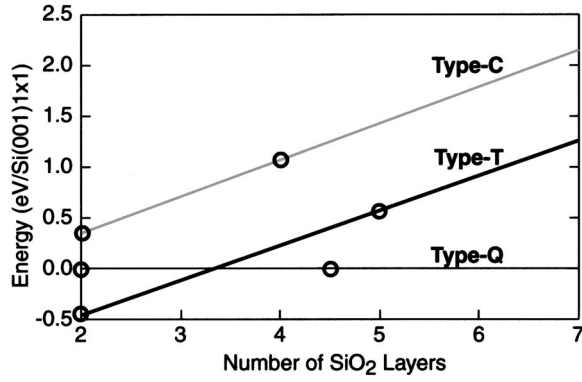


FIG. 3. Relative energies of type-*C*-, *T*-, and *Q*-structures, where the energy of the 2-ML type-*Q* structure is set to be a basis. Small circles plotted on lines are the points where we have the actual total energies.

essarily claim that thick oxides take a type-*Q* structure. Whether the type-*T* structure still remains near the interface or the phase changes completely to a type-*Q* structure is an open question.

We simulated x-ray-diffraction patterns for the three thick crystalline SiO₂ structures. All of them could not reproduce the specific (1 1 0.45) peak observed by Shimura *et al.*¹ The type-*Q* structure has a strong intensity at an index of (1 1 0.62). Thus the slight rearrangement of the Si-O network in the type-*Q* structure, to elongate the periodicity along the direction normal to the interface, can possibly explain the peak intensity of the experimental value.

Our Si(001)/SiO₂ interfacial models, which were presented in this paper, have only one kind of suboxide of Si²⁺ at the interface, whereas multiple suboxide states of Si¹⁺, Si²⁺, and Si³⁺ are observed to coexist by photoemission spectroscopy.^{14–16} As for the distribution of these suboxides, experimental results spread in a wide range from a few atomic layers to more than ten.^{14–16} However, when the oxide films are grown on well-prepared atomically flat Si(001) subsurfaces, most experimental results show that the suboxide region is confined within a few monolayers.¹⁶ Moreover, a recent experiment¹⁷ demonstrated that the oxidation can be processed layer by layer without introducing additional roughness via careful choices of oxidation conditions. Thus our abrupt interfacial model is an idealized one, but is not oversimplified from the real interface, considering the every effort toward the formation of smooth interface in the modern Si technology.

Finally, we investigate the effective band-gap variation in the vicinity of the interface by using the local density of states (LDOS's). We divide the unit cell into 1.0 a.u. (=0.529 Å) thick slices parallel to the interface, and specify each slice as a local (μ th) region Ω_μ , and then define a local density of states $D_\mu(\epsilon)$ of the μ th region as

$$D_\mu(\epsilon) = \frac{1}{V_{BZ}} \sum_\nu \int \omega_{k\nu}^\mu \delta(\epsilon - \epsilon_{k\nu}) dk, \quad (1)$$

$$\omega_{k\nu}^\mu = \int_{\Omega_\mu} \rho_{k\nu}(\mathbf{r}) d\mathbf{r}, \quad (2)$$

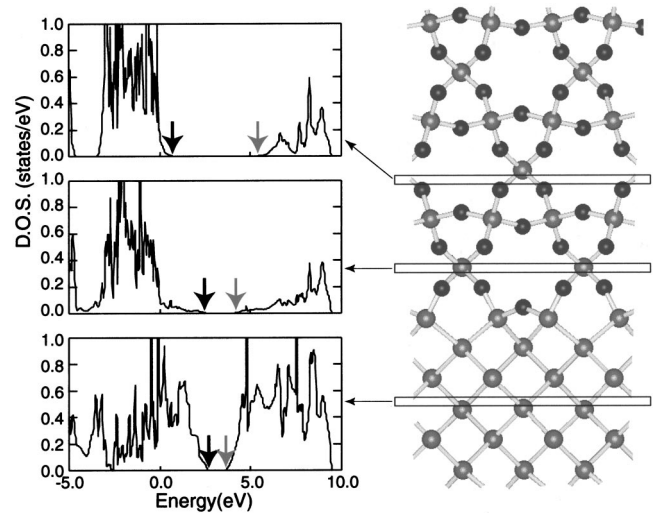


FIG. 4. LDOS's for three representative local regions; namely, deep substrate, the vicinity of the interface, and deep SiO₂, in the 4.5-ML type-*Q* structure. Black and shaded arrows denote the energies of the valence-band maxima and conduction-band minima, respectively. On the right-hand side, we show the geometric structure, with local sliced regions corresponding to LDOS graphs on the left-hand side. Black and gray balls are oxygen and silicon atoms, respectively.

where \mathbf{k} denotes a point in the Brillouin zone, ν is a band index, V_{BZ} is the volume of the Brillouin zone, and $\rho_{k\nu}(\mathbf{r})$ is a partial electron density contributed from an eigenwave function labeled by \mathbf{k} and ν . The integration with respect to \mathbf{k} in Eq. (1) is evaluated with a tetrahedron method using 25 \mathbf{k} points in the Brillouin zone. Figure 4 shows several representative LDOS's for the thick type-*Q* model. LDOS's in the substrate Si region commonly show that the band gap is as small as about 1 eV.¹⁸ In deep SiO₂ regions (>5 Å), the LDOS's show wide band gaps comparable to that of bulk quartz of 5.8 eV. We define the conduction-band minimum (CBM) and the valence-band maximum (VBM) by using the criteria

$$\int_{V_{BZ}} D_\mu(\epsilon) d\epsilon = \int_{E_F}^{CBM} D_\mu(\epsilon) d\epsilon = \Delta \int_{-\infty}^{E_F} D_\mu(\epsilon) d\epsilon, \quad (3)$$

with $\Delta = 0.001$. The values of the CBM and VBM depend on the choice of Δ . However, as demonstrated in Fig. 4, the CBM and VBM marked by arrows clearly correspond to the effective edges of the LDOS.

In Fig. 5 we plot the CBM and VBM along the normal direction for a type-*Q* structure. Other structures show similar behaviors. An energy-gap change occurs in the SiO₂ layer, and is almost complete at about 5 Å deep from the interface.¹⁹ The CBM and VBM variations along the normal direction of the interface models have specific features. The CBM varies rather gradually in the transition region. The variation of the VBM is different from that of the CBM. The VBM in a SiO₂ region between the interface and a point about 2 Å deep from the interface retain almost the same values as those in the Si substrate. From this point, the VBM starts to decrease rapidly, and almost saturates at 5 Å. There

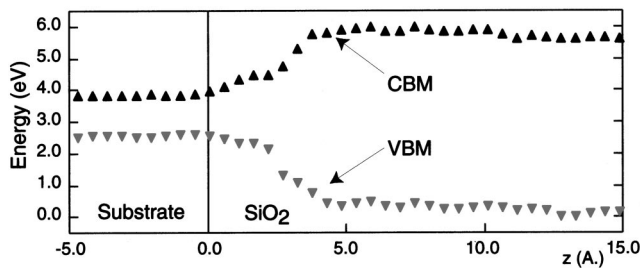


FIG. 5. Variation of the VBM and CBM along the normal direction to the interface for the 4.5-ML type- Q structure. The position of the topmost silicon of the substrate is set to be the origin of the distance.

is 2–5-Å-thick transition region on the SiO_2 side. These features are common in other interfacial structures of types T and C . Muller *et al.*²⁰ observed ultrathin gate oxides with atomic-scale electron-energy-loss spectroscopy, and found that the two interface systems of c - $\text{Si}/\text{SiO}_2/a$ - Si have 4.5–7.5-Å-thick transition regions. They also observed that the ellipsometric thickness of the SiO_2 region is thinner by

3–6 Å than the geometric one. These experimental features are consistent with our theoretical results. These features of the transition region should be taken into account for designing MOS devices, especially when holes are used as carriers.

IV. SUMMARY

We examined the stability of the three interface structure models for thin (2 ML) and thick (4–5 ML) cases. When the oxide layers are thinner than ~ 3 ML, the tridymite structure is the most stable. When the oxide layers exceeds ~ 4 ML, the most stable structure is the quartz type. The pseudocristobalite structure is unfavorable for all range of thickness because of the large lattice mismatch. The local density of states shows that an effective band-gap change occurs on the SiO_2 side within 5 Å from the interface.

ACKNOWLEDGMENTS

We thank Dr. Awaji for giving us an x-ray simulation program. We also acknowledge NEDO, who provided us a chance to use a vector parallel computer VPP500 and VPP700 introduced into JRCAT.

*Present address: Matsushita Research Institute Tokyo, 3-10-1 Higashimita, Tama-Ku, Kawasaki 214, Japan.

¹T. Shimura, H. Misaki, M. Umeno, I. Takahashi, and J. Harada, *J. Cryst. Growth* **166**, 786 (1996).

²I. Takahashi, T. Shimura, and J. Harada, *J. Phys.: Condens. Matter* **5**, 6525 (1993).

³A. Ourmazd, D. W. Taylor, J.A. Rentschler, and J. Berk, *Phys. Rev. Lett.* **59**, 213 (1987).

⁴F. Rochet, M. Froment, C. D'Anterroches, H. Roulet, and G. Dufour, *Philos. Mag. B* **59**, 339 (1989).

⁵S. Carniato, G. Boureau, and J. Harding, *Radiat. Eff. Defects Solids* **134**, 179 (1995).

⁶A. Pasquarello, M.S. Hybertsen, and R. Car, *Appl. Phys. Lett.* **68**, 625 (1996).

⁷H. Kageshima and K. Shiraishi, *Appl. Surf. Sci.* **176**, 130 (1998).

⁸R. Buczko, S.J. Pennycook, and S.T. Pantelides, *Phys. Rev. Lett.* **84**, 943 (2000).

⁹D. Vanderbilt, *Phys. Rev. B* **41**, 7892 (1990).

¹⁰J.P. Perdew, in *Electronic Structure of Solids '91*, edited by P. Ziesche and H. Eschrig (Akademie Verlag, Berlin, 1991).

¹¹N. Binggeli, N. Trullier, J.L. Martins, and J.R. Chelikowsky, *Phys. Rev. B* **44**, 4771 (1991).

¹²We have optimized the lattice constants and atomic coordinates

of the bulk counterpart, and found that the total energy is higher than that of the α quartz by 0.14 eV per SiO_2 unit. The value is comparable with that of the cubic faujasite (one of the zeolite family) (Ref. 13), which suggests the existence of a SiO_2 phase in nature.

¹³I. Petrovic, A. Navrotsky, M.E. Davis, and S.I. Zones, *Chem. Mater.* **5**, 1805 (1993).

¹⁴P.J. Grunthaner, M.H. Hecht, and F.J. Grunthaner, *J. Appl. Phys.* **61**, 629 (1987).

¹⁵F.J. Himpsel, F.R. McFeely, A. Taleb-Ibrahimi, J.A. Yarmoff, and G. Hollinger, *Phys. Rev. B* **38**, 6084 (1988).

¹⁶T. Aiba, K. Yamauchi, Y. Shimizu, N. Tate, M. Katayama, and T. Hattori, *Jpn. J. Appl. Phys.* **34**, 707 (1995).

¹⁷H. Watanabe, K. Kato, T. Uda, K. Fujita, M. Ichikawa, T. Kawamura, and K. Terakura, *Phys. Rev. Lett.* **80**, 345 (1998).

¹⁸This band-gap value of 1 eV is larger compared to the ordinary obtained value for bulk Si using DFT, which is an effect of the quantum confinement due to the limitation of substrate thickness.

¹⁹C. Kaneta, T. Yamasaki, T. Uchiyama, T. Uda, and K. Terakura, *Microelectronic Eng.* **48**, 117 (1999).

²⁰D.A. Muller, T. Sorsch, S. Moccio, F.H. Baumann, K. Evans-Lutterodt, and G. Timp, *Nature (London)* **399**, 758 (1999).